Generalized Quadrature Spatial Modulation aided Millimetre Wave MIMO

Reba P[1], Janani Nanthakumar[2], Jaisri A[3], Shunmuga Bhagya Shri T[4], Swathi S[5]
Dept. of Electronics and Communication Engineering
PSG Institute of Technology and Applied Research
Coimbatore, India
rebasatheesh@gmail.com[1], jananikumar1998@gmail.com[2], armsri56484@gmail.com[3], shunmugabhagyashri6@gmail.com[4], sswathika99@gmail.com[5]

Abstract— **Millimetre wave (mm-wave) communication and Multiple Input Multiple Output (MIMO) systems are promising solutions to overcome the challenge possessed by the future wireless systems. Spatial Modulation (SM) techniques has the inherent potential to overcome the drawbacks of MIMO systems such as increased energy consumption, complexity and cost. Quadrature Spatial Modulation (QSM) is another type of spatial modulation technique and it helps in enhancing the spectral efficiency achieved by Spatial Modulation (SM) by transmitting additional base 2 logarithm of N_t bits and it retains all other advantages of SM. A novel Generalized QSM (GQSM) aided mm-wave MIMO structure is proposed in this paper. In order to select the antenna combinations in GQSM a virtual antenna grouping is performed. The analytical and simulated average BER of the proposed system are compared to analyse its performance. Also, the average BER performance of the proposed system outperforms the GSM aided mm-wave MIMO and QSM aided mm-wave MIMO systems.**

Keywords— Millimeter wave, MIMO, Spatial Modulation, Quadrature Spatial Modulation

I. INTRODUCTION

Millimetre Wave (mm-wave) communication is strongly recognized as the key technique to increase Spectral Efficiency (SE) to support 5G communication networks [1]. Millimetre wave frequency range spans from 3 GHz to 300 GHz and offers large bandwidth and hence solves the problem of spectral congestion. Multiple Input Multiple Output (MIMO) systems has been proved as a promising technology which supports increase in capacity and reliability of wireless communications and are currently being used in 4G systems [2],[3]. Combining mm-wave with MIMO communications, facilitates the overall increase in data rate. In MIMO systems, RF chains are connected to each antenna. This increases the hardware cost and its complexity. Furthermore, signal transmitted from all the antennas at the same time and frequency causes severe Inter Channel Interference (ICI) [4].

Spatial Modulation (SM) technique was introduced to overcome such challenges [5], [6]. SM is an energy efficient scheme and uses only one RF chain, thus reducing the complexity and cost of the hardware. In SM, the information bits are divided into two blocks. One block of bits act as the spatial symbols and it is used to select the antennas whereas, the other block of bits is converted to symbols and transmitted through the selected antennas. Since only one antenna is chosen, ICI and ISI are avoided. Also, the total number of antennas (N_t) required for SM must be a power of 2. Furthermore, the SE achieved by SM ($\eta_{SM} = log_2 N_t + log_2 M$) is less than that achieved by the spatial multiplexing system where the data rate increases linearly with the number of transmit antennas. To overcome the above limitations, Generalized SM (GSM) is proposed in [7], where the spatial symbols select more than one transmit antennas. Since multiple antennas are selected for transmission, the SE is increased in GSM compared to SM.

Quadrature Spatial Modulation (QSM) [8] is another type of SM, where the real and imaginary parts of the complex data symbol is simultaneously transmitted through one or 2 antennas depending on the spatial symbols. The spectral efficiency of QSM is, $\eta_{QSM} = 2 \times log_2 N_t + log_2 M$. Thus, it has $log_2 N_t$ bits improvement in SE than SM. Also, orthogonal carriers are used to transmit the in-phase and Q-phase signals in different antennas. Hence the ICI is avoided.

Generalised Complex QSM (GCQSM) technique is proposed in [9], where the authors explained two methods GQSM – with unique combinations (GQSM-UC) and GQSM-with permuted combinations (GQSM-PC).The authors claimed that the number of transmit antennas required for attaining the same SE is reduced when compared with other SM methods. In [10], the authors proposed two methods for GQSM: 1) Modified GQSM (mGQSM) and 2) Reduced Codebook mGQSM (RC-mGQSM). In the first method a novel codebook is designed and it achieves a 1 bit increase in SE. The second method aims at reducing the complexity but the achievable SE get reduced. [11] explains a GQSM system based on antenna grouping and they assumed 2 antennas per group. The spectral efficiency of the proposed technique is increased compared to other conventional schemes. But, from the spatial constellation, it can be seen that for most of the spatial bits both the antennas are active. This increases the hardware cost and complexity. In [12], the authors present a GQSM scheme for large scale MIMO system. They also proposed an antenna selection scheme to reduce the computational complexity overhead. In all these works ([9] to [12]) GQSM in mm-wave massive MIMO context is not explained.

Average BER comparison of SM and spatial multiplexing for mm-wave outdoor channel model is provided in [13]. In [14] the authors proposed a complete structure of GSM aided transmitter for mm-wave MIMO communications. [15] explains QSM for outdoor mm-wave communication. The mutual information and the achievable capacity of mm-wave QSM system is derived. However, the structure of the mm-wave communication transmitter for QSM is not explained. In [16] QSM for massive MIMO systems is explained. Here the massive MIMO transmitting antennas are split into groups and QSM is applied to each groups in parallel. The SE of this Parallel QSM (PQSM) is increased compared to QSM. However, this increases the complexity in detection of PQSM at the receivers. Moreover the complete structure of massive MIMO transmitter is not explained.

978-1-7281-7299-6/20/$31.00 ©2020 IEEE

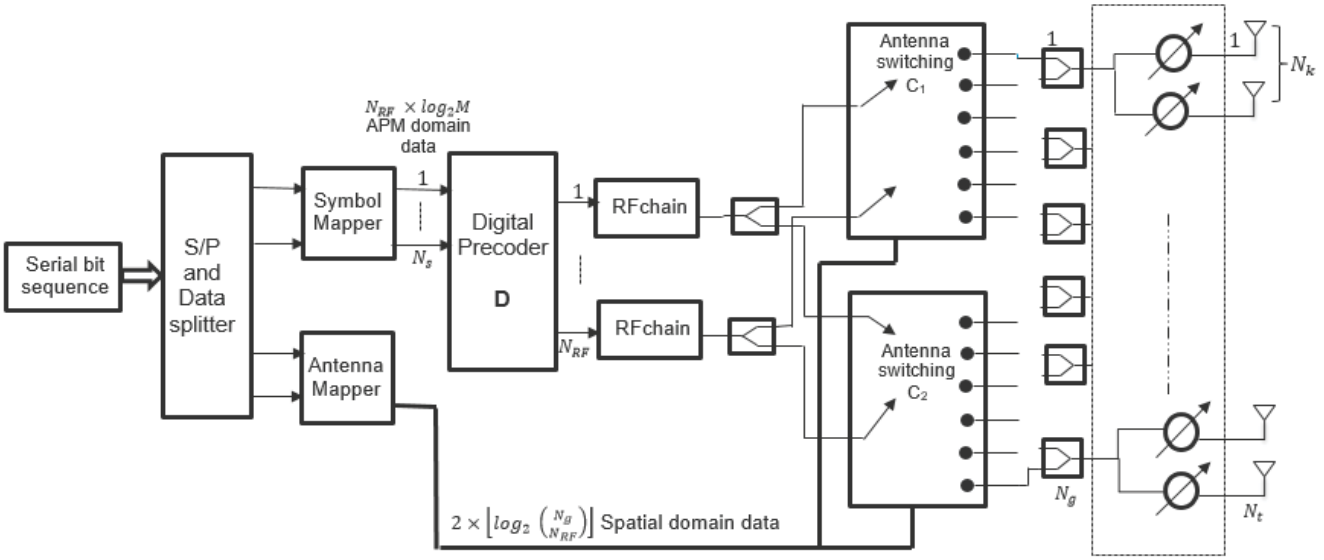

Fig. 1 Transmitter structure of GQSM aided mm-wave MIMO system

Mapping Table T_2	
Bits	Active Antenna groups
0 0 0	(1,4)
0 0 1	(1,5)
0 1 0	(1,6)
0 1 1	(2,4)
1 0 0	(2,5)
1 0 1	(2,6)
1 1 0	(3,5)
1 1 1	(3,6)

Mapping Table T_1	
Bits	Active Antenna groups
0 0 0	(1,4)
0 0 1	(1,5)
0 1 0	(1,6)
0 1 1	(2,4)
1 0 0	(2,5)
1 0 1	(2,6)
1 1 0	(3,5)
1 1 1	(3,6)

Fig. 2 Antenna Mapping Tables

In this paper GQSM for mm-wave MIMO with complete transmitter and receiver structure is proposed. In our proposed method, the assignment of antenna combinations to spatial domain bits assume a virtual grouping of antennas. This proposed method is much less complex than the PQSM method [16]. The average BER performance of the proposed method is analysed and it is compared with GSM aided mm-wave MIMO [14] and QSM for mm-wave [15]. The average BER of the proposed GQSM is less than that of [14] and [15].

The remainder of this paper is organized as follows; section II describes the system model. The proposed GQSM aided mm-wave MIMO is discussed in section III. Section IV presents the simulation results, comparing the performance of the proposed schemes which is followed by conclusion of this work in section V.

Notation: Matrices and Vectors are denoted by boldface uppercase and boldface lowercases respectively. $\|\mathbf{A}\|$, $\|\mathbf{v}\|_2$ represents frobenius norm of a matrix $\mathbf{A}$ and ℓ^2 -norm of a vector v respectively. $\mathbf{I}_M$ represents M × M identity matrix. E[.] represents the statistical expectation operator, $Pr\{.\}$ represents probability. det(.), Tr(.), $(.)^{-1}$and $(.)^{\dagger}$ denotes the determinant, trace, inverse and conjugate transpose operations. diag ([**x**]) represents diagonal matrix with vector $\boldsymbol{x}$ along the diagonal.

II. System Model

Consider a mm-wave MIMO system with N_t transmit antennas and N_r receive antennas. The incoming bit streams are split into two groups viz. APM domain data bits and spatial domain bits. The APM domain data bits are converted into N_s number of symbols based on the APM constellation chosen and then they are processed by the digital precoder $\boldsymbol{D}$. The digital precoder converts the N_s symbols to N_{RF} RF domain symbols. The size of the digital precoder is $N_{RF} \times N_s$. The in-phase and Q-phase outputs of RF chains are connected separately to the selected antenna combinations based on both, the spatial domain bits and the antenna bits mapping tables - T_1 and T_2.

Moreover, in the mm-wave MIMO structure considered, the N_t transmit antennas are divided into N_g groups and each group has N_k number of antennas. Hence $N_t = N_k N_g$. Therefore, based on the space domain information as well as the mapping of tables T_1 and T_2, the symbols from RF chains are connected to antenna group combinations. In order to select the antenna groups, high speed mm-wave RF switches with low insertion loss and high isolations are used.

If there are L number of different antenna combinations there will be L number of digital precoders $\{\boldsymbol{D}_1, \boldsymbol{D}_2 \dots \dots \boldsymbol{D}_L\}$. These matrices are real valued diagonal matrices. Hence based on the spatial domain data bits and instantaneous CSI, one of the digital precoders is chosen. The digital precoding is performed in digital domain and hence it is easy to switch to different $\boldsymbol{D}_i$ based on the spatial domain data bits.

The N_k antennas in each groups are connected to phase shifters. Thus, there are a total of N_t phase shifters and they correspond to analog precoding in mm-wave MIMO systems. The analog precoding matrix is a diagonal matrix of dimension $N_t \times N_t$ and it is defined as,

$$\boldsymbol{A} = diag\left(\frac{1}{\sqrt{N_k}} e^{j\psi_1}, \frac{1}{\sqrt{N_k}} e^{j\psi_1}, \dots \dots \dots \frac{1}{\sqrt{N_k}} e^{j\psi_{N_t}}\right) \quad (1)$$

The received signal $\boldsymbol{y} \in \mathbb{C}_{N_r \times 1}$ at the input of the receiver is given by,

$$\boldsymbol{y} = \sqrt{\rho}\, \boldsymbol{H}\, \boldsymbol{A}\, \boldsymbol{C}_m \boldsymbol{D}_m \boldsymbol{s} + \boldsymbol{n} \quad (2)$$

$\boldsymbol{s} \in \mathbb{C}_{N_s \times 1}$ is the input signal vector from APM domain input data bits, ρ is the average transmit power, $\boldsymbol{n} \in \mathbb{CN}\left(0, \sigma_n^2 I_{N_r}\right)$ is the additive White Gaussian noise at the receivers. $\boldsymbol{C}_m$ is the $N_t \times N_{RF}$ antenna selection matrix. In order to characterize the mm-wave MIMO channel model, Saleh-Valenzuela geometric channel model [12] is used.

$$\boldsymbol{H} = \sqrt{N_r N_t} \sum_{p=1}^{N_{cl}} \sum_{q=1}^{N_{ray}} (\alpha_{pq} \Lambda_t(\phi_{pq}^t, \theta_{pq}^t) \Lambda_r(\phi_{pq}^r, \theta_{pq}^r) \times \boldsymbol{b}_t(\phi_{pq}^t, \theta_{pq}^t) \mathbf{b}_r(\phi_{pq}^r, \theta_{pq}^r)) \quad (3)$$

N_{cl}, N_{ray} are the no of scattering clusters and the no of paths per cluster. $\alpha_{pq} \in \mathbb{C}(0, \sigma^2)$ is the channel gain. $\phi_{pq}^r(\theta_{pq}^r), \phi_{pq}^t(\theta_{pq}^t)$ is the azimuth (elevation) angles of arrival and departure respectively. $\Lambda_r(\ ), \Lambda_t(\ )$ represent the receive and transmit antenna gain. $\boldsymbol{b}_t(\phi_{pq}^t, \theta_{pq}^t), \mathbf{b}_r(\phi_{pq}^r, \theta_{pq}^r)$ is the transmit and receive array response vector.

III. GQSM FOR MM-WAVE MIMO

Fig. 1 shows the proposed GQSM for mm wave MIMO. GQSM selects more than one transmit antenna based on the spatial domain bits and the number of RF chains. Generally, in SM techniques, a mapping table which provides the mapping information about all the possible spatial domain bits and their respective antenna combinations, is available at the transmitter. In the proposed system, instead of selecting the transmit antennas from the set $\{1,2 \ldots\ldots N_t\}$, transmit antenna groups are selected from the antenna group set $\{1,2 \ldots\ldots N_g\}$. Each group has N_k no of antennas. Virtual

Furthermore, a different way of antenna group selection is followed in the proposed method. The antenna groups are divided further based on the number of RF chains available. For example, if the available number of RF chains (N_{RF}) is 2 and the number of antenna groups N_g is 6, then among the 6 antenna groups, 2 antenna groups are selected for transmission. Also, instead of selecting the random antenna groups (like, $(1,2), (3,4)\ etc.$) , the total number of antenna groups are divided into two sets (since $N_{RF} = 2$). Antenna groups $\{1,2\ and\ 3\}$ belong to the first set and the remaining antenna groups $\{4,5\ and\ 6\}$ belong to the second set. Now, the new antenna group combinations are $\{(1,4), (1,5), (1,6), (2,4), (2,5)\ etc.\}$ i.e. each antenna group in the combinations are selected from the different sets. The antenna mapping tables are shown in Fig.2. Thus, this method of selecting antenna groups helps in reducing the Inter Channel Interference (ICI), since no two immediate neighbouring antenna groups are selected for transmission at the same time.

The antenna group mapping tables for in-phase and Q-phase symbols T_1, T_2 respectively is shown in the Fig.2. Correspondingly, the antenna selection matrices are $C_1\ and\ C_2$ respectively. The size of C_1 and C_2 is $N_t \times N_{RF}$. Assume $N_t = 12$, $N_k = 2, N_g = 6, N_{RF} = 2$ and C_1 corresponds to $(2,4)$ from mapping table T_1 and C_2 corresponds to $(3,5)$ from mapping table T_2. Then C_1 and C_2 antenna selection matrices can be written as,

$$C_1 = \begin{bmatrix} 0 & 0 & 1 & 1 & 0 & 0 & 0 & 0 & 0 & 0 & 0 & 0 \\ 0 & 0 & 0 & 0 & 0 & 0 & 1 & 1 & 0 & 0 & 0 & 0 \end{bmatrix}^T \quad (4)$$

$$C_2 = \begin{bmatrix} 0 & 0 & 0 & 0 & 1 & 1 & 0 & 0 & 0 & 0 & 0 & 0 \\ 0 & 0 & 0 & 0 & 0 & 0 & 0 & 0 & 1 & 1 & 0 & 0 \end{bmatrix}^T \quad (5)$$

The number of bits required to choose N_{RF} number of antenna groups from the total N_g antenna groups is $\left\lfloor log_2 \binom{N_g}{N_{RF}} \right\rfloor$ bits. Since in GQSM, separate antenna group combinations are needed to transmit the in-phase and Q-phase components, the total no of bits required to represent the spatial domain data is $2 \times \left\lfloor log_2 \binom{N_g}{N_{RF}} \right\rfloor$.

Let M be the constellation size of APM domain data bits. Since N_{RF} antenna groups are selected, each group will carry independent APM data symbols. Therefore the no. of bits required to represent the APM domain data is, $N_{RF} \times log_2 M$. Hence the achievable spectral efficiency of GQSM is given by,

$$\eta_{GQSM} = \underbrace{2 \times \left\lfloor log_2 \binom{N_g}{N_{RF}} \right\rfloor}_{2 \times k\ bits} + \underbrace{N_{RF} \times log_2 M}_{N_{RF} \times b\ bits} \quad bpcu \quad (6)$$

A. GQSM transmission Scheme:

1. First the $N_{RF} \times b\ bits$ of the incoming bit stream are converted in to N_{RF} APM symbols chosen from M-QAM constellation given by,

$$\begin{aligned} x_1 &= x_{\Re_1} + j x_{\Im_1} \\ x_2 &= x_{\Re_2} + j x_{\Im_2} \\ &\vdots \\ x_{N_{RF}} &= x_{\Re_{N_{RF}}} + j x_{\Im_{N_{RF}}} \end{aligned} \quad (7)$$

2. These symbols are processed by the digital precoders followed by the in-phase and Q-phase modulation based RF chain. The N_{RF} RF symbols are given by,

$$\begin{aligned} s_1(t) &= x_1 \times e^{j2\pi f_c t} \\ s_2(t) &= x_2 \times e^{j2\pi f_c t} \\ &\vdots \\ s_{N_{RF}}(t) &= x_{N_{RF}} \times e^{j2\pi f_c t} \end{aligned} \quad (8)$$

3. The next k bits of the incoming bit stream are used to select one of the antenna group combinations based on the information from table T_1 to transmit the real part of the APM domain symbols. Assume, $s_{\Re_1}, s_{\Re_2}, \ldots\ldots s_{\Re_{N_{RF}}}$ are the real part of $s_1(t), s_2(t), \ldots s_{N_{RF}}(t)$ then the transmitted signal vector is $\boldsymbol{s}_{\Re} = [s_{\Re_1}, s_{\Re_2}, \ldots\ldots s_{\Re_{N_{RF}}}]^T$. Let $\ell_{\Re_1}, \ell_{\Re_2}, \ldots\ldots \ell_{\Re_{N_{RF}}}$ are the indices of the antennas selected and $\boldsymbol{C_1}$ is the antenna selection matrix

4. Similarly the subsequent k bits of the incoming bit stream are used to select one of the antenna group combinations based on the information from table T_2 to transmit the imaginary part of the APM domain symbols. Assume, $s_{\Im_1}, s_{\Im_2}, \ldots\ldots s_{\Im_{N_{RF}}}$ are the imaginary part of $s_1(t), s_2(t), \ldots s_{N_{RF}}(t)$, then the transmitted signal vector is $\boldsymbol{s}_{\Im} = [j s_{\Im_1}, j s_{\Im_2}, \ldots\ldots j s_{\Im_{N_{RF}}}]^T$. Let $\ell_{\Im_1}, \ell_{\Im_2}, \ldots\ldots \ell_{\Im_{N_{RF}}}$ are the indices of the antennas selected and $\boldsymbol{C_2}$ is the antenna selection matrix

The received signal at the GQSM mm-wave MIMO receiver is given by,

$$\boldsymbol{y} = \sqrt{\rho}\,\boldsymbol{H}\,\boldsymbol{A}\,\sum_{i=1}^{2}\boldsymbol{C}_i\boldsymbol{D}_i\boldsymbol{s}_i \quad + \boldsymbol{n} \tag{9}$$

where, $\boldsymbol{s}_1 = \boldsymbol{s}_{\Re}$ and $\boldsymbol{s}_2 = \boldsymbol{s}_{\Im}$. Thus the real and imaginary components are combined and then transmitted. The design of hybrid precoders is not the scope of this paper. Hence we assume that,

$$\boldsymbol{A} = \boldsymbol{I}_{N_t}\ ,\quad \boldsymbol{D}_i = \boldsymbol{I}_{N_s} \tag{10}$$

If $\boldsymbol{C}_1$ and $\boldsymbol{C}_2$ are given by equation (4) and (5), then, $\boldsymbol{C}_1\boldsymbol{s}_1 = \begin{bmatrix}0 & 0 & s_{\Re_1} & s_{\Re_1} & 0 & 0 & s_{\Re_2} & s_{\Re_2} & 0 & 0 & 0 & 0\end{bmatrix}^T$. Similarly, $\boldsymbol{C}_2\boldsymbol{s}_2 = \begin{bmatrix}0 & 0 & 0 & 0 & js_{\Im_1} & js_{\Im_1} & 0 & 0 & js_{\Im_2} & js_{\Im_2} & 0 & 0\end{bmatrix}^T$. The actual RF signal transmitted is, $\boldsymbol{C}_1\boldsymbol{s}_1 + \boldsymbol{C}_2\boldsymbol{s}_2$ and it is normalized by $\sqrt{4}$ (in this case). For certain bit combinations, both in-phase and quadrature phase signals get transmitted through the same antenna, in such cases, a RF combiner is needed at each RF terminals to combine both in-phase and Q-phase.

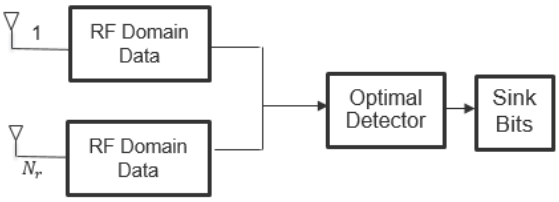

Fig. 3. Receiver structure of GQSM system

B. GQSM Reception:

At the receiver, the Maximum Likelihood (ML) detection principle is used to jointly decode the spatial symbol and the data symbol.

$$\left[\tilde{\ell}, \tilde{s}\right] = arg\min_{\ell,\boldsymbol{s}}\|\boldsymbol{y} - \boldsymbol{H}\boldsymbol{s}\|^2 \tag{11}$$

The Pair wise Error Probability (PEP) is given by,

$$Pr_{error} = \Pr\left(\left(\boldsymbol{h}_{\ell_{\Re}}, \boldsymbol{h}_{\ell_{\Im}}, \boldsymbol{s}_i\right) \rightarrow \left(\boldsymbol{h}_{\tilde{\ell}_{\Re}}, \boldsymbol{h}_{\tilde{\ell}_{\Im}}, \boldsymbol{s}_{\tilde{\imath}}\right)/\boldsymbol{H}\right) \tag{12}$$

$$= Pr\left(\left\|\boldsymbol{y} - \left(\boldsymbol{h}_{\ell_{\Re}}s_{\Re} + \boldsymbol{h}_{\ell_{\Im}}s_{\Im}\right)\right\|^2 > \left\|\boldsymbol{y} - \left(\boldsymbol{h}_{\tilde{\ell}_{\Re}}s_{\tilde{\Re}} + \boldsymbol{h}_{\tilde{\ell}_{\Im}}s_{\tilde{\Im}}\right)\right\|^2/\boldsymbol{H}\right)$$

$$= Pr(2\,Re\{n^H\boldsymbol{\Psi}\} > \|\boldsymbol{\Psi}\|^2/\boldsymbol{H})$$

where, $\boldsymbol{\Psi} = \left(\left(\boldsymbol{h}_{\ell_{\Re}}s_{\Re} - \boldsymbol{h}_{\tilde{\ell}_{\Re}}s_{\tilde{\Re}}\right) + \left(\boldsymbol{h}_{\ell_{\Im}}s_{\Im} - \boldsymbol{h}_{\tilde{\ell}_{\Im}}s_{\tilde{\Im}}\right)\right)$

Therefore,

$$Pr_{error} = Q\left(\sqrt{\frac{\|\boldsymbol{\Psi}\|^2}{2\sigma^2}}\right) \tag{13}$$

$$= Q\left(\sqrt{snr^{QSM}}\right) \tag{14}$$

The average PEP is given as,

$$\mathrm{E}[Pr_{error}] = \frac{1}{2}\left(1 - \sqrt{\frac{\mathrm{E}[snr^{QSM}]/2}{1+\mathrm{E}[snr^{QSM}]/2}}\right) \tag{15}$$

The upper bound on BER derived based on union bounding technique is,

$$Avg\ BER = \frac{1}{2^{\eta_{GQSM}}}\sum_{\ell,s}\sum_{\tilde{\ell},\tilde{s}}\frac{b_{\tilde{\ell},\tilde{s}}^{\ell,s}}{\eta_{GQSM}}\left(\mathrm{E}[Pr_{error}]\right)^{N_r}\sum_{i=0}^{N_r-1}\binom{N_r-1+i}{i}\left[1 - \mathrm{E}[Pr_{error}]\right]^i \tag{16}$$

where, $\ell \in \{\ell_{\Re}, \ell_{\Im}\}$ and $b_{\tilde{\ell},\tilde{s}}^{\ell,s}$ is the no of bits in error.

C. Complexity Analysis:

In this section the receiver complexity in terms of number of real multiplications for the proposed GQSM is compared with PQSM [16]. The optimum receiver for GQSM is given by (11). The complexity of this receiver is,

$$2^{\eta_{GQSM}}4N_r(N_{RF} + 1) \tag{17}$$

where, $2 \times 2N_{RF}$ real multiplications are needed for computing $\boldsymbol{hs}$. Another 4 real multiplications are needed for computing $|\ |^2$. These computations are repeated for $N_r 2^{\eta_{GQSM}}$ times.

The receiver complexity of QSM is, $8N_r 2^{\eta_{GQSM}}$, and the receiver complexity for PQSM is $8PN_r 2^{\eta_{GQSM}}$, where P is the number of parallel groups considered. Thus, the proposed receiver complexity of GQSM mm-wave MIMO is less than that of PQSM technique.

IV. Simulation Results

In this section, we study the analytical and simulation results of the proposed GQSM technique for mm-wave MIMO systems. Monte-Carlo simulations with 10000 channel realizations are used to compare the performance of the GQSM techniques for mm-wave MIMO systems. The parameters used for mm-wave MIMO system simulation are based on [14]. It is assumed that both the transmit antennas and receive antennas are uniform linear array antennas with spacing $d = \lambda$.

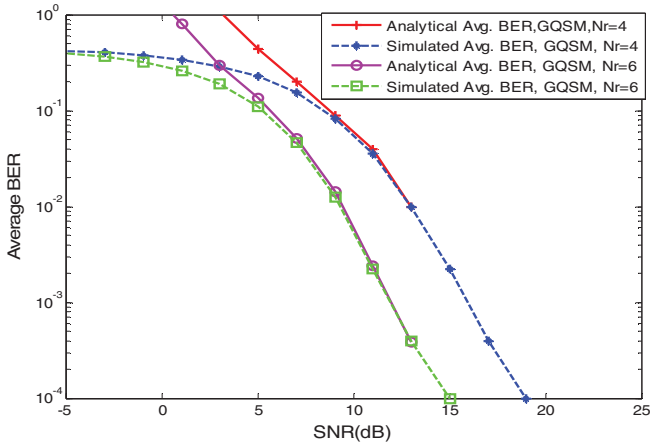

Fig. 4 Average BER performance of GQSM with ($N_r = 4, 6$), $N_t = 12$, $N_g = 6$, $N_{RF} = 2$, $M = 4$ and Spectral Efficiency = 10 bits.

Fig. 4 shows the analytical and simulated graphs of the average BER versus the SNR of the proposed GQSM technique for varying no. of receive antennas ($N_r = 4$ and $N_r = 6$). The spectral efficiency assumed is 10 bits for both the cases. The other parameters are $N_t = 12$, $N_g = 6$, $N_{RF} = 2$,$M = 4$ along with a 4 QAM Modulation. Here, each RF chain carries different symbols. From the figure, it can be seen that the simulated results tightly follow the average BER upper bound. Moreover, with an increase in the number of receive antennas, the average BER reduces by 4 dB.

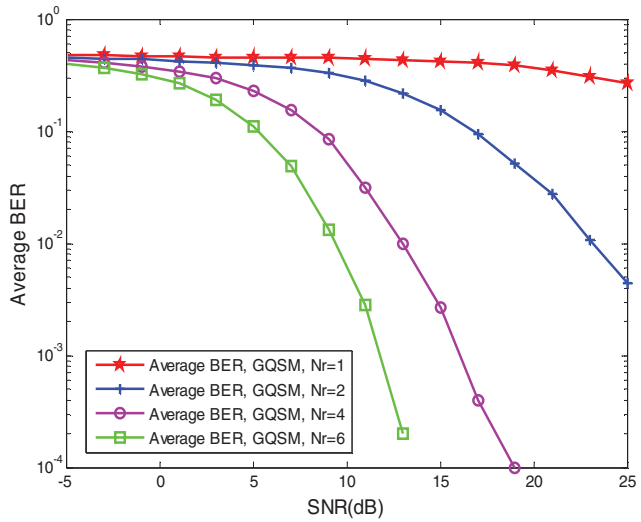

Fig. 5 Comparison of simulated average BER performance of GQSM against SNR with different receive antennas ($N_r = 1,2,4,6$), $N_t = 12$, $N_g = 6$, $N_{RF} = 2$,$M = 4$ and Spectral Efficiency= 10 bits.

Fig. 5 shows the comparison of the simulated version of the average BER for different no of receive antennas (Nr=1,2,4 and 6) with respect to the SNR. The other parameters remain the same as in the first case. As the number of receive antennas increases, the wrong detection of spatial bits decreases and hence the BER increases.

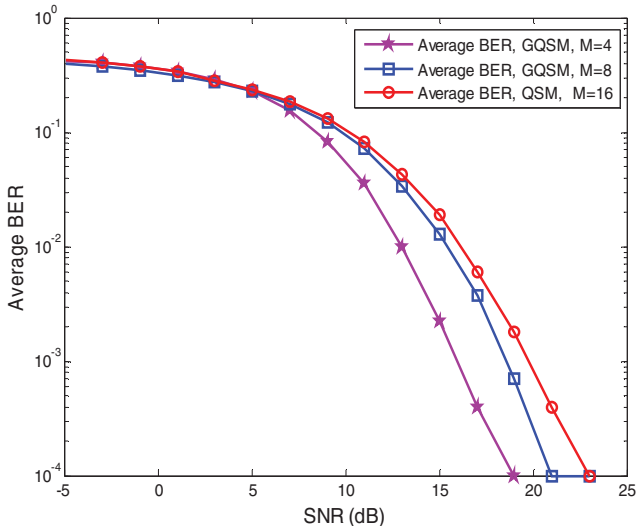

Fig. 6 - Comparison of average BER performance of GQSM ($M = 4, 8$) and with QSM system ($M = 16$), spectral efficiency = 10 bits.

Fig 6 shows the comparison of the performance of the GQSM for different system configurations. The spectral efficiency is fixed for all the three configurations shown in the figure and it is equal to 10 bits. The other parameters considered for GQSM system with $M = 4$ are $N_t = 12$, $N_g = 6$, $N_r = 4$, $N_{RF} = 2$, where, each RF chain carries different APM symbols chosen from a constellation of size M=4. The parameters considered for GQSM system with M=8 are $N_t = 8$, $N_g = 4$, $N_r = 4$, $N_{RF} = 2$ and each RF chain carries different APM symbols chosen from a constellation of size M=8. Both the system configurations result in a spectral efficiency of 10 bits. It can be observed from the figure that the average BER performance of GQSM system with $N_t = 12$ outperforms the one with $N_t = 8$. This is because $N_t = 8$ requires a larger symbol constellation size than that of $N_t = 12$ and hence it causes more symbol detection errors.

This figure also compares the performance of proposed GQSM system with the QSM system for a spectral efficiency of 10 bits. The other parameter considered for QSM system is, $N_t = 16$, $N_g = 8$, $N_r = 4$, $N_{RF} = 1$ and the RF chain carries one APM symbol chosen from the constellation of size M=16. It is observed from the figure that QSM system results in larger BER than the GQSM system. This is because in GQSM system the number of RF chains is more than that of the QSM system. This reduces the constellation size of GQSM system by mapping more bits to spatial domain than to APM domain. Thus, the decrease in constellation size in GQSM system when compared to QSM system leads to larger Euclidean distance between the APM symbols in the APM domain and yields lower average BER.

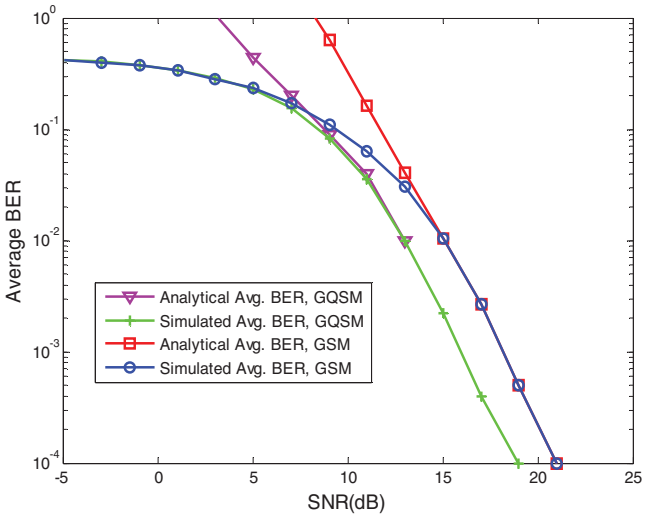

Fig. 7 - Comparison of average BER performance of GQSM and with GSM system, spectral efficiency = 10 bits.

Fig. 7 compares the average BER achieved by proposed GQSM system and GSM system for spectral efficiency of 10 bits. The GQSM system considers, $N_t = 12$, $N_g = 6$, $N_r = 4$, $N_{RF} = 2$ and $M = 4$. The system parameters considered for GSM system is $N_t = 8$, $N_g = 4$, $N_{RF} = 2$, $N_r = 4$ and $M = 16$. In GQSM system and GSM system, both RF chains carry different symbols from their respective APM domain constellation. The above figure shows that the average BER performance of proposed GQSM system outperforms GSM system. For an average BER of 10^{-3}, the GQSM shows 2dB gain over the GSM system. The reason is that in GQSM systems more bits are mapped to spatial domain rather than APM domain whereas in GSM system only less bits are mapped to spatial domain. Thus a larger constellation size is needed to represent the APM domain bits in GSM system and this leads to more average BER compared to GQSM system.

V. Conclusion

In this paper we propose a GQSM transceiver structure for mm-wave MIMO system. In the proposed method a different antenna selection scheme is followed to avoid ICI. We analyse the performance of the proposed system in terms of average BER. The average BER performance of the proposed system is also compared with that of QSM and GSM aided mm-wave MIMO. Simulation results show that the proposed GQSM mm-wave MIMO system achieves reduction in average BER compared to that of other schemes. Also the complexity of the proposed GQSM mm-wave MIMO is less when compared to that of the PQSM technique.

REFERENCES

[1] S. Rangan, T. S. Rappaport and E. Erkip, "Millimeter-wave cellular wireless networks: Potentials and challenges", Proc. IEEE, vol. 102, no. 3, pp. 366-385, Mar. 2014.

[2] T. S. Rappaport et al., "Millimeter wave mobile communications for 5G cellular: It will work!", IEEE Access, vol. 1, pp. 335-349, May 2013.

[3] R. Paul Sam and U. M. Govindaswamy, "Antenna selection and adaptive power allocation for IA-based underlay CR," IET Signal Processing, vol. 11, no. 6, pp. 734-742, August 2017.

[4] P. Reba, G. Umamaheswari and G. Suchitra, "Performance Investigation of Interference Alignment Techniques for Underlay MIMO Cognitive Radio Networks," 2018 15th IEEE India Council International Conference (INDICON), Coimbatore, India, 2018, pp. 1-5.

[5] D. A. Basnayaka, M. Di Renzo and H. Haas, "Massive but few active MIMO", IEEE Trans. Veh. Technol., vol. 65, no. 9, pp. 6861-6877, Sep. 2016.

[6] M. Wen *et al*., "A Survey on Spatial Modulation in Emerging Wireless Systems: Research Progresses and Applications," IEEE Journal on Selected Areas in Communications, vol. 37, no. 9, pp. 1949-1972, Sept. 2019.

[7] A. Younis, N. Serafimovski, R. Mesleh and H. Haas, "Generalised spatial modulation," 2010 Conference Record of the Forty Fourth Asilomar Conference on Signals, Systems and Computers, Pacific Grove, CA, 2010, pp. 1498-1502.

[8] R. Mesleh, S. S. Ikki and H. M. Aggoune, "Quadrature spatial modulation", IEEE Trans. Veh. Technol., vol. 64, no. 6, pp. 2738-2742, Jun. 2015.

[9] Manar Mohaisen, "Generalized Complex Quadrature Spatial Modulation", Hindawi Wireless Communications and Mobile Computing, Volume 2019.

[10] K. Gunde and K. V. S. Hari, "Modified Generalised Quadrature Spatial Modulation," 2019 National Conference on Communications (NCC), Bangalore, India, 2019, pp. 1-5.

[11] Francisco Ruben Castillo-Soria, Joaqun Cortez-Gonzalez, Raymundo Ramirez-Gutierrez, Fermın Marcelo Maciel-Barboza, and Leonel Soriano-Equigua, "Generalized Quadrature Spatial Modulation Scheme Using Antenna Grouping", ETRI Journal, Vol.39, pp. 707-717, October 2017.

[12] Atoyebi Bolajoko Arikea , Abdulsalam Khadeejah Adebisib , Babatunde Olubayo Mosesc, "Complex Generalized Quadrature Spatial Modulation for Large Scale MIMO System Jordan Journal of Electrical Engineering", Vol. 5, No. 1, pp 1-10, 2019

[13] Salma Elkawafi, Abdelhamid Younis, Raed Mesleh, Abdulla Abouda, Mohammed Elmusrati and Ahmed Elbarsha, "Spatial Modulation and Spatial Multiplexing Performance Comparison Over 3D mmWave Communications", IEEE WiSPNET 2017 conference

[14] L. He, J. Wang and J. Song, "On Generalized Spatial Modulation Aided Millimeter Wave MIMO: Spectral Efficiency Analysis and Hybrid Precoder Design," IEEE Transactions on Wireless Communications, vol. 16, no. 11, pp. 7658-7671, Nov. 2017.

[15] Abdelhamid Younis, Nagla Abuzgaia, Raed Mesleh, and Harald Haas, "Quadrature Spatial Modulation for 5G Outdoor Millimeter–Wave Communications: Capacity Analysis", IEEE Trans. on Wireless Comm., Vol. 16, no. 5, May 2017

[16] G. Huang, C. Li, S. Aïssa and M. Xia, "Parallel Quadrature Spatial Modulation for Massive MIMO Systems with ICI Avoidance," IEEE Access, vol. 7, pp. 154750-154760, 2019.